

Published in final edited form as:

Nature. 2012 July 12; 487(7406): 231–234. doi:10.1038/nature11180.

## Independent evolution of striated muscles in cnidarians and bilaterians

Patrick R.H. Steinmetz<sup>1</sup>, Johanna E.M. Kraus<sup>1</sup>, Claire Larroux<sup>2,3</sup>, Jörg U. Hammel<sup>4</sup>, Annette Amon-Hassenzahl<sup>5</sup>, Evelyn Houlston<sup>6</sup>, Gert Wörheide<sup>3,7,8</sup>, Michael Nickel<sup>4,7</sup>, Bernard M. Degnan<sup>2</sup>, and Ulrich Technau<sup>1,#</sup>

<sup>1</sup>Department for Molecular Evolution and Development, Centre for Organismal Systems Biology, University of Vienna, Althanstraße 14, A-1090 Vienna, Austria

<sup>2</sup>Centre for Marine Science, School of Biological Sciences, The University of Queensland, Brisbane Queensland 4072, Australia

<sup>3</sup>Department of Earth and Environmental Sciences, Palaeontology & Geobiology, Ludwig-Maximilians-Universität München, Richard-Wagner-Str. 10, 80333 München, Germany

<sup>4</sup>Institut für Spezielle Zoologie und Evolutionsbiologie mit Phyletischem Museum, Friedrich-Schiller-Universität Jena, Erbertstraße 1, D-07743 Jena, Germany

<sup>5</sup>Institute of Zoology, Technical University of Darmstadt, Schnittspahnstraße 10, 64287, Darmstadt, Germany

<sup>6</sup>Université Pierre et Marie Curie and CNRS, “Biologie du Développement” UMR 7009, 06230 Villefranche-sur-Mer, France

<sup>7</sup>GeoBio-Center, Ludwig-Maximilians-Universität München, Richard-Wagner-Str. 10, 80333 München, Germany

<sup>8</sup>Bayerische Staatssammlung für Paläontologie und Geologie, Richard-Wagner-Str. 10, 80333 München, Germany

### Abstract

Striated muscles are present in bilaterian animals (e.g. vertebrates, insects, annelids) and some non-bilaterian eumetazoans (i.e. cnidarians and ctenophores). The striking ultrastructural similarity of striated muscles between these animal groups is thought to reflect a common evolutionary origin<sup>1, 2</sup>. Here we show that a muscle protein core set, including a Myosin type II Heavy Chain motor protein characteristic of striated muscles in vertebrates (MyHC-st), was already present in unicellular organisms before the origin of multicellular animals. Furthermore, *myhc-st* and *myhc-non-muscle* (*myhc-nm*) orthologues are expressed differentially in two

---

#Corresponding author: Ulrich.technau@univie.ac.at.

#### Author contributions

PS and UT designed the study, analysed data, and wrote the paper. PS performed the bioinformatic and phylogenetic analyses, most *N.v.* experiments and cloned two *Aq-myhc* genes. JK performed and analysed all *C.h.* experiments. CL cloned all *T.w.* genes and performed all *in situ* hybridisation experiments on *T.w.* and *A.q.* JH and MN performed SEM and sectioning of *T.w.* animals. AAH cloned the *Nv-myhc-st* gene and performed *in situ* hybridisation and sectioning experiment of adult *N.v.* GW and EH provided unpublished EST sequences, and EH helped performing *C.h.* experiments. MN, CL, GW, and JH analysed the *T.w.* data, and CL and BD analysed the *A.q.* data.

#### Author information

Reprints and permissions information is available at [www.nature.com/reprints](http://www.nature.com/reprints).

The authors declare no competing financial interests.

Supplementary Information is linked to the online version of the paper at [www.nature.com/nature](http://www.nature.com/nature)

sponges, compatible with the functional diversification of *myhc* paralogues before the origin of true muscles and the subsequent deployment of *MyHC-st* in fast-contracting smooth and striated muscle. Cnidarians and ctenophores possess *myhc-st* orthologues but lack crucial components of bilaterian striated muscles, such as *tropomyosin* complex and *titin* genes, suggesting the convergent evolution of striated muscles. Consistently, jellyfish orthologues of a shared set of bilaterian z-disc proteins are not associated with striated muscles, but are instead expressed elsewhere or ubiquitously. The independent evolution of eumetazoan striated muscles through the addition of novel proteins to a pre-existing, ancestral contractile apparatus may serve as a paradigm for the evolution of complex animal cell types.

## Results and discussion

Cnidarians and bilaterians<sup>1, 3-5</sup>, as well as a single ctenophore species<sup>6</sup>, share smooth and striated muscle cell types, which are absent in other non-bilaterian phyla (i.e. sponges and placozoans). The characteristic striation is due to the reiteration of a contractile unit, the sarcomere, composed of alternating assemblies of myosin-based thick filaments and actin-based thin filaments, bordered by the supporting z-discs<sup>3, 7, 8</sup>. The strong ultrastructural similarities of striated muscles are highly suggestive of a common evolutionary origin<sup>1, 2</sup> but independent origins have been discussed<sup>4, 5</sup>. We have reassessed muscle evolution by genome mining and molecular phylogenetic approaches coupled with expression analysis in sponges and cnidarians. A comparative analysis of 47 bilaterian muscle components in 22 completely sequenced genomes of species representing metazoans, closest-related protists, fungi, and representatives of other eukaryotic groups allowed us to reconstruct key steps in muscle evolution (Fig.1, Supplementary Fig.1). First, we identified a core set of contractile proteins that predates muscle evolution and is conserved amongst metazoans, holozoan protists, fungi and amoebozoans (Fig. 1a and Supplementary Fig. 1a,b). This set comprises actin, myosin type II heavy chain (MyHC) and their associated proteins (Myosin light chains, Tropomyosin and Calmodulin). Presumably, this actomyosin machinery fulfilled basic cytoskeletal roles (e.g. cell division or shape changes) in the common ancestor of these various multi- and unicellular organisms before adopting additional roles in muscle contraction during animal evolution. Second, we identified Myosin light chain kinase (MLCK) as a metazoan innovation, which allowed for the tight regulation of actomyosin contraction by coupling Regulatory Light Chain (RLC) phosphorylation to elevated cytoplasmic Ca<sup>2+</sup> concentrations in muscle and non-muscle cells<sup>9, 10</sup> (Supplementary Fig. 1b,d). Notably, all associated regulatory components, except Caldesmon, are present in all animals (Fig.1a, Supplementary Fig. 1b). Hence, of the different known modes of muscle contraction regulation<sup>9</sup>, MLCK-dependent RLC phosphorylation appears most ancient. A third major finding is that not one of the 47 structural or regulatory proteins we analysed is uniquely shared between cnidarians and bilaterians, i.e. no protein correlates with the evolutionary origin of muscle. These observations suggest that the core contractile apparatus in eumetazoan muscles antedates the origin of the animal kingdom and that lineage-specific innovations underlie muscle evolution in cnidarians and bilaterians.

Previous studies suggested that a gene duplication event gave rise to two distinct phylogenetic groups of *myhc* orthologues in bilaterian animals, each having a distinct function and pattern of expression<sup>11-13</sup>. Bilaterian “non-muscle” orthologues (MyHC-nm) function during common cellular processes (e.g. cell division or migration) and during vertebrate smooth muscle contraction<sup>14</sup>, while bilaterian “muscle” orthologues (MyHC-st) function specifically in vertebrate striated muscles and in both smooth and striated muscles of protostomes<sup>15</sup>. Counter-intuitively, our analyses demonstrate that the gene duplication that generated the two MyHC orthology groups occurred much earlier than the origin of muscle cells (Fig.2, Supplementary Fig.2). Bilaterians, cnidarians, ctenophores, placozoans

and sponges (the latter two lacking muscles) each possess at least one of each MyHC-nm and MyHC-st orthologues with specific coiled-coil domain structures, while the unicellular organisms *Capsaspora owczarzaki*, *Sphaeroforma arctica* and choanoflagellates possess a clear member of the MyHC-nm group, characterized by a specific coiled-coil structure (except in the reduced choanoflagellate MyHCs) (Fig.2, Supplementary Fig.2). The tree topology strongly indicates that the *myhc-st* and *myhc-nm* genes had already separated in the last common ancestor of all animals and the aforementioned protists, with the latter having later lost *myhc-st* (Fig.2, Supplementary Figs. 1d, 2).

To address how *myhc-st* and *myhc-nm* are used in non-bilaterian animals, we investigated their deployment in two sponges, generally considered to lack muscles, as well as two cnidarian species harbouring striated and smooth muscles (Fig.3, Supplementary Figs. 3-6). In *Tethya wilhelma*, a demosponge, *myhc-nm* expression was detected in a wide variety of cell types (Supplementary Fig. 3a-g) including the pinacocytes, primarily responsible for the peristalsis-like contractions of the adult sponge<sup>16</sup> (Supplementary Fig. 3e). In contrast, *Tw-myhc-st* expression is restricted to the outlet pore (apopyle) of the current-producing choanocyte chambers (Fig. 3a,c, Supplementary Fig. 3h-k), the site of a sieve-like cell type (Fig. 3b,c and Supplementary Fig. 4) proposed to regulate the water flow<sup>17</sup>. In larvae of the demosponge *Amphimedon queenslandica*, the *myhc* orthologues were found differentially expressed in regions of presumptive cell shape change or migration<sup>18</sup>, with *Aq-myhc-nm* more broadly expressed than *Aq-myhc-st* (Supplementary Fig.5). We conclude that the segregation of a “general function” *myhc-nm* orthologue, and a more specialised *myhc-st* orthologue had already occurred in the last common ancestor of demosponges and all other animals, accounting for their evolutionary retention over long times.

In cnidarians, we found *myhc-st* orthologs prominently expressed in fast-contracting muscle cells, but also in a few non-muscle cell types. In the sea anemone *Nematostella vectensis* (with smooth muscles only), *myhc-st* (formerly termed *Nv-myhc1*<sup>19</sup>) is strongly expressed in the tentacle and body column retractor muscles that contract oral-aborally during escape response (Fig. 3d-k). *Nv-myhc-nm* on the other hand is broadly expressed in the whole endoderm, hence in all endodermal epitheliomuscular cells (Supplementary Fig. 6a-c). In the hydrozoan *Clytia hemisphaerica*, *myhc-st* expression is detected in the developing striated ring muscles of the velum and the subumbrella (Fig. 3l-r; Supplementary Fig. 6g-k) that propel the medusa by fast contractions. It is further detected in the tentacles and the mouth tube ectoderm (manubrium)(Fig. 3n,r), which both include longitudinal smooth muscles. *Ch-myhc-nm*, like *Nv-myhc-nm*, is expressed broadly in the endoderm including the smooth muscle-rich gastrovascular system, and in non-muscle cells of the tentacle bulb nematocyte precursor region (Supplementary Fig. 6d-f). Thus, in both cnidarian species examined, *myhc-st* is predominantly expressed in fast-contracting muscles while the broad *myhc-nm* expression includes smooth and non-muscle cell types. A clear segregation of function between a muscle- and a more general-purpose MyHC is thus observed, albeit less pronounced than in bilaterians.

MyHC-st is the predominant motor protein in all striated muscles so far investigated, but its deployment in smooth retractor muscles in *Nematostella* shows that it is not sufficient to confer striation. We therefore examined the presence of other striated muscle components in cnidarians. A hallmark of striated muscle regulation and formation in bilaterians is the Troponin complex, comprising Troponin I, C and T<sup>9, 20</sup>. To our surprise, none of the corresponding genes could be found in the genome sequences of the non-bilaterian species, the cnidarians *Nematostella vectensis*, *Acropora digitifera* or *Hydra magnipapillata*, the ctenophore *Mnemiopsis leidyi*, the placozoan *Trichoplax adherens*, or in the deeply sequenced transcriptome of *Clytia hemisphaerica* medusae (Fig. 1a, Supplementary Fig.

1a,d), indicating that muscle striation or the regulation of contraction are not Troponin-dependent in these organisms.

Concerning components of the z-disc<sup>21-23</sup>, a marked lack of conservation was discovered even within the Bilateria. Nearly half of the known vertebrate (13 out of 28) and a quarter of the known *Drosophila melanogaster* (2 out of 8) z-disc proteins<sup>21-23</sup> are uniquely present (Fig. 1b) or have unique protein domain structures (Supplementary Fig. 7a,e; 8a) in either chordates or *D. melanogaster*. Of the remaining proteins, only 4 orthologue groups localise to the z-disc in both taxa: the actin-scaffolding protein  $\alpha$ -Actinin, its binding partners Muscle-Lim and Ldb3/Zasp, and the giant Titin proteins, which regulate sarcomeric length and integrity (Fig. 1b). Thus, a considerable part of the complex vertebrate and insect z-disc interactomes evolved by the recruitment of novel, lineage-specific proteins to a “proto-z-disc” complex of only 4 proteins present in their last common ancestor (Supplementary Fig. 1c).

Of the four “proto-z-disc” components, only the general, hence uninformative, cellular actin cross-linker *a-actinin* is expressed during striated muscle formation in jellyfish *MuscleLim* and *ldb3/zasp*, like *a-actinin*, originated before animal evolution (Fig. 1b, Supplementary Figs. 1c, 7b-d). Their expression was not, however, detected in developing or differentiated striated muscles in *C. hemisphaerica* medusae (compare Fig. 4a-f and Fig. 3m,n,q,r), but rather was concentrated in endodermal radial canals and other endodermal structures (Fig. 4). Similarly, *Nv-ldb3/zasp* and *Nv-muscleLim*<sup>24</sup> gene expression was detected throughout the endoderm (Supplementary Fig. 10) and therefore in all types of smooth epithelial muscle cells except the ectodermal tentacle retractor muscles. Titin appears absent in non-bilaterians, as Immunoglobulin / Fibronectin type III (Fn)-domain super-repeats, characteristic of the giant Titin proteins<sup>25, 26</sup> were not identified in any predicted proteins from non-bilaterian genomes (Fig. 1b, Supplementary Figs. 8b,c).

Proteins found in the z-discs of *Drosophila melanogaster* but so far not in the vertebrate z-discs appear to be absent outside Bilateria. Amongst vertebrate z-disc components not detected in *D. melanogaster* z-discs, many play general roles in the cytoskeleton (*capZ- $\alpha$* , *capZ- $\beta$* , *lasp*), signal transduction (*calcineurin A* and *calcineurin B*) or protein degradation (*trim9/67* ubiquitin ligase). Orthologues of these genes are expressed ubiquitously in *C. hemisphaerica* (Supplementary Fig. 9) and in *N. vectensis* (Supplementary Fig. 11). Finally, Obscurin, a giant sarcomeric protein anchored in vertebrate but not the *Drosophila* z-discs and predominantly expressed in striated muscles of vertebrates, flies and nematodes<sup>27</sup> is expressed throughout all tissue layers of *C. hemisphaerica* (Supplementary Fig. 9g) and in the smooth muscle-forming *N. vectensis* endoderm (Supplementary Fig. 11kk-mm), suggesting a more general role in cnidarians.

To conclude, we have shown that cnidarians lack all molecular hallmarks of bilaterian striated muscles except *myhc-st* expression, and thus striated muscles in Bilateria and Hydrozoa are very likely to have evolved convergently from cells with an ancient contractile machinery (Supplementary Fig. 1d). This may also apply to the striated muscles of the ctenophore *Euplokamis sp.*<sup>4, 6</sup>, as suggested by their isolated occurrence within the ctenophores. We suggest that the observed correlation between *myhc-st* expression and striated muscles in bilaterians and hydrozoan jellyfish is due to functional constraints: MyHC-st-based “bipolar” thick filaments (as found in vertebrate and protostome striated muscles) may favour a faster contraction and reiteration of the acto-myosin machinery when compared with MyHC-nm-based “side-polar” thick filaments (as found in vertebrate smooth and non-muscle cells)<sup>28</sup>. Our work revealed that the origin of many components integral to muscle cell function (notably MyHC-st) predates that of muscle cells, while others (such as the Troponin complex, Paramyosin or Titin) were acquired progressively during muscle

specialisations in different animal groups (Supplementary Fig. 1d). A similar scenario may also apply to other complex cell types. Our analysis of striated muscle evolution therefore highlights that ultrastructural similarity alone is not a reliable indication of common evolutionary origin, but can be achieved independently by different sets of proteins.

## Methods summary

Details of animal husbandry, genome mining, protein domain structure, phylogenetic and expression analyses, cloning, microscopy and image processing are found in Methods.

## Methods

### Animal culture and collection

*Nematostella vectensis* was cultured and gametogenesis induced as described<sup>43</sup>. *Clytia hemisphaerica* was cultured as described previously<sup>44</sup> but using artificial sea salt (Red Sea, Erkrath, Germany). Adult specimens of *Amphimedon queenslandica* were collected on Heron Island Reef, Great Barrier Reef, Australia as previously described<sup>45</sup>. Adult specimens of *Tethya wilhelma* were collected from aquaria of the Zoologisch-Botanischer Garten Wilhelma, Stuttgart<sup>46</sup> and cultured as previously described<sup>16,47</sup>.

### BLAST searches

A reference set of 46 muscle proteins from mouse, human or *Drosophila melanogaster* was compiled from in-depth literature searches and searched in the publically available, fully sequenced genomes of *Branchiostoma floridae*<sup>48</sup>, *Capitella teleta*, *Nematostella vectensis*<sup>49</sup>, *Hydra magnipapillata*<sup>50</sup>, *Mnemiopsis leidy*<sup>51</sup>, *Trichoplax adhaerens*<sup>52</sup>, *Amphimedon queenslandica*<sup>53</sup>, *Monosiga brevicollis*<sup>54</sup>, *Salpingoeca rosetta*<sup>55</sup>, *Capsaspora owczarzakii*<sup>55</sup>, *Allomyces macrogynus*<sup>55</sup>, *Spizellomyces punctatus*<sup>55</sup> and *Thecamonas trahens*<sup>55</sup>, *Chlamydomonas reinhardtii*<sup>56</sup>, *Selaginella moellendorffii*<sup>57</sup>, *Dictyostelium discoideum*<sup>58</sup>, *Naegleria gruber*<sup>59</sup>, *Phanerochaete chrysosporium*<sup>60</sup>, *Saccharomyces cerevisiae* and *Schizosaccharomyces pombe*<sup>61</sup> (and for confirmation of gene absence in *Helobdella robusta* and *Lottia gigantea*) by reciprocal BLASTP and TBLASTN using the web-interface BLAST pages of the Joint Genome Institute (JGI) (<http://genome.jgi-psf.org/> or <http://www.phytozome.net/>), the Metazome platform (<http://spongezome.metazome.net/> or <http://hydrazome.metazome.net/>), the NCBI BLAST platform (<http://www.ncbi.nlm.nih.gov/blast/>), the GeneDB website of the Wellcome Trust Sanger Institute (<http://old.genedb.org/genedb/pombe/>), the Saccharomyces genome database (<http://www.yeastgenome.org/>), the Origins of Multicellularity Sequencing Project, Broad Institute of Harvard and MIT ([http://www.broadinstitute.org/annotation/genome/multicellularity\\_project/MultiHome.html](http://www.broadinstitute.org/annotation/genome/multicellularity_project/MultiHome.html)), or deeply sequenced transcriptomic data of early developmental stages and adult medusae of *Clytia hemisphaerica* (JK, UT and EH). *Mnemiopsis* genomic contigs were searched by TBLASTN using the NCBI BLAST software package. The coding sequence of the hits on *M. leidy* contigs was identified by using Genscan<sup>62</sup>. Absences in *H. magnipapillata* and *N. vectensis* further confirmed by searching deep sequencing transcriptomic data of *C. hemisphaerica* planula and medusa stages (JK, UT and EH), EST sequences available from *Acropora millepora* and *Metridium senile* EST sequences through GenBank, and the *Acropora digitifera* genome<sup>63</sup>. Genomes were blasted using BLASTP or TBLASTN using pre-set parameters (BLOSUM62 matrix, expected e-value threshold: 10 (local), 0.1 (Metazome), 1e-3 (Broad) or 1e-5 (JGI)). In case no similar protein could be found with expected e-values <1, the BLAST was repeated using an expected e-value threshold of 1. The first hits were reciprocally blasted using the BLASTP algorithm of the NCBI BLAST server (<http://blast.ncbi.nlm.nih.gov/Blast.cgi>) against the “nr” database and further analysed by protein domain and phylogenetic analysis.

In case no similar hit was found in non-metazoan genomes, BLAST searches were repeated using a previously identified cnidarian or sponge protein sequence. The *Clytia hemisphaerica* transcriptomic sequencing data covered 41.7 Mb in 24663 unigenes, with a median length of 1.3 kb, mean of 1.7 kb and maximum transcript length of 25 kb. The *Tethya wilhelma* EST data covered 12.1 Mb in 29660 unigenes, with a median length of 379 bp, mean of 407 bp and maximum transcript length of 3006 bp.

### Protein domain structure analysis

Protein domain structures were analysed using the HMMPfam, HMMSmart and HMMPanther applications of the InterProScan platform at the EBI, Hinxton (<http://www.ebi.ac.uk/Tools/pfa/iprscan/>)<sup>64</sup>. Better visualisation of longer proteins was obtained using Pfam online tools<sup>65</sup> (Wellcome Trust Sanger Institute, <http://pfam.sanger.ac.uk/>). Coiled-coil domain structure predicted using the COILS<sup>66</sup> ([http://www.ch.embnet.org/software/COILS\\_form.html](http://www.ch.embnet.org/software/COILS_form.html)).

### Phylogenetic analysis

All protein multiple sequence alignments performed using MUSCLE v.3.6<sup>67</sup>. Sequence stripping with GBLOCKS<sup>68</sup> using the least conservative parameters (Min. Num. of Seq. for Flank Pos.: lowest possible; Min. Block Length: 2; Gaps settings: None for MyHC (choanoflagellates, *Hydra magnipapillata* & *Clytia hemisphaerica*, Paramyosin,). No gaps included: Calcineurin A. Half gaps included: MyHC (full lengths, Fig. 3), Ldb3/Zasp,  $\alpha$ -Actinin, Muscle Lim, Calcineurin B and TRIM/MuRFs. All Gaps: Four-and-a-half-Lim, Stripped alignments were tested for the best fitting maximum likelihood parameters using Prottest v2.4 and excluding HIV and mitochondrial substitution matrices<sup>69</sup>. Neighbour-joining trees calculated using the built-in algorithm of ClustalX (using correction for multiple substitutions)<sup>70</sup>. Maximum likelihood trees calculated using PhyML v.3.0 for MacOS<sup>71</sup> using a BioNJ input tree, optimised tree topology, 4 substitution rate categories, “median” as middle of each rate class, SPR topological moves and 100 non-parametric bootstrap replicates. Model of amino acid substitutions and additional parameters: LG+I+G except for Four-and-a-half-LIM and Muscle Lim (both WAG+I+G) and for Calcineurin B (LG+G). Bayesian trees calculated with a parallel version of MrBayes 3.1.2<sup>72, 73</sup>.

### Cloning of cnidarian and sponge genes

Novel transcripts were amplified from cDNA or identified from EST libraries. Fragments of *Nv- $\alpha$ -actinin*, *Nv-calcineurin A*, *Nv-calcineurin B*, *Nv-capZ $\alpha$* , *Nv-capZ $\beta$* , *Nv-lasp1*, *Nv-lasp2*, *Nv-lasp3*, *Nv-limpet*, *Nv-obscurin*, *Nv-muscleLim1.1*, *Nv-muscleLim1.2*, *Nv-muscleLim2*, *Nv-ldb3/zasp*, *Nv-myhc-st*, *Nv-mhc-nm*, *Ch-myhc-nm*, *Ch-myhc-st*, *Ch-ldb3/zasp*, *Ch-muscleLim*, *Ch- $\alpha$ -actinin*, *Ch-calcineurin A*, *Ch-capZ $\alpha$* , *Ch-capZ $\beta$* , *Ch-lasp*, *Ch-limpet*, *Ch-obscurin* and *Ch-trim9/6/7*, *Aq-myhc-st*, *Aq-myhc-nm*, *Tw-myhc-nm1*, *Tw-myhv-nm2*, *Tw-myhc-st1*, *Tw-myhc-st2* were identified as EST fragment clones or newly cloned by designing primers for predicted genes based on the *Nematostella vectensis* genome assembly 1.0, the *Amphimedon queenslandica* genome assembly or *Clytia hemisphaerica* and *Tethya wilhelma* transcriptomics data (see also Supplementary Table 1).

### Whole-mount in situ hybridisation (WMISH)

WMISH was performed as previously described for *N. vectensis*<sup>74</sup> and *A. queenslandica*<sup>75, 76</sup>. For *C. hemisphaerica*, the *N. vectensis* protocol was modified using 10 minutes of 0.1  $\mu$ g/ml Proteinase K (Ambion, Austin, TX) at 37°C and hybridised at 60°C (*Ch-ldb3/zasp* and *Ch-muscleLIM*) or 63°C (all other genes). As multiple splice variants of *Ch-ldb3/zasp* were found, a 5'RACE fragment containing the N-terminal PDZ domain, a crucial  $\alpha$ -actinin-binding motif found also in all vertebrate Ldb3/Zasp isoforms, was chosen

to perform *in situ* hybridisations. For *Tethya wilhelma*, sponges were removed from the culture mesh, settled in a glass dish (1-2 weeks), and prevented from merging with each other. Just prior to fixation, the dish containing sponges was removed from the aquarium and sponge contraction was inhibited by incubation for 15 min at 25°C in 10% Listerine mouthwash (Johnson & Johnson, New Brunswick, NJ). Sponges were scrapped off the dish, rapidly transferred into a 6-well plate containing fixative, fixed as previously described<sup>75, 76</sup> with a fixative change after 5 min, and transferred to screwcap tubes of 70% ethanol for -20°C storage. For WMISH, the *A. queenslandica* protocol<sup>75, 76</sup> was modified by skipping proteinase K digestion, acetylation, and post-fixation. For paraffin embedding, WMISH samples were dehydrated in an 7-step increasing graded series of ethanol, transferred into HistoClear through an intermediate step of ethanol/HistoClear (1:1). Following several changes of HistoClear at room temperature, specimens were incubated in HistoClear/Paraplast (1:1) at 42° C for 1 hour, followed by 48 hours in Paraplast at 58° C with regular total replacement of the Paraplast every 12 hours. Samples were subsequently embedded into Paraplast at room temperature and sectioned at 7 µm after hardening using a Microm HM360. Serial sections were transferred to slides, cleared from Paraplast using HistoClear and mounted in Euparal.

### Light and confocal microscopy

All light microscopy pictures were done with Nikon Eclipse E80 and an Olympus BH2, both equipped with DIC optics and a Zeiss AxioCam. All confocal microscopy pictures were done with a Leica TCS SP5 X.

### Scanning electron microscopy

*Tethya wilhelma* sample in Fig. 3 was fixed in a 0.45 M sodium acetate buffer (pH 6.4 in filtered aquarium seawater) + 2% OsO<sub>4</sub> + 2% glutaraldehyde + 0.29 M sucrose immediately after sampling, desilified in 5% hydrofluoric acid for 1 h and then embedded in styrene-methacrylate<sup>77, 78</sup>. After semi-thin sectioning on a Microm HM360, remaining plastic was removed using xylene-treatment and the samples dehydrated in increasing acetone concentrations. Specimens were critically point dried in an Emitech K850 CPD system (Ashford, Great-Britain) and sputter coated in an Emitech K500 SC system (Ashford, Great-Britain). SEM images were taken on a Philips XL30ESEM. *Tethya wilhelma* sample in Supplementary Fig. 5 was prepared as described before<sup>16, 34</sup>. In brief, specimens were shock-frozen in liquid N<sub>2</sub>, fractured and subsequently fixed by freeze-substitution in a Leica AFS (Leica, Bensheim, Germany) in MeOH with 1% OsO<sub>4</sub>, 2.5% glutaraldehyde and 2.5% distilled water at -80° C for 68.5 h, followed by heating to 0° C at a constant rate of 40° C per hour. Samples were completely dehydrated and critical point dried with liquid CO<sub>2</sub> in a Balzers CPD (Balzers Union, Neugruet, Switzerland) and sputtered with Gold in an Emitech K500 (Ashford, Great-Britain). Specimens were investigated in a digital Zeiss DSM 940A (Zeiss Oberkochen, Germany) scanning electron microscope at 5–20 kV.

### Image processing software

WMISH images were cropped, adjusted for levels, brightness, contrast and color balance using Adobe Photoshop CS2 (Adobe, San Jose, California). Stacks of light microscopy focal planes were assembled with Helicon Focus Software (Kharkov, Ukraine). All schematics and panels were designed with FreeHand MX (Adobe, San Jose, California).

### Supplementary Material

Refer to Web version on PubMed Central for supplementary material.

## Acknowledgments

For access and use of publicly available, unpublished enome sequences, we thank the “Origins of Multicellularity Sequencing Project, Broad Institute of Harvard and MIT (<http://www.broadinstitute.org/>), the JGI as well as Alexis Baxevanis (NIH) and Joe Ryan (Sars Centre Bergen). We thank Maja Adamska (Sars Centre, Bergen) for providing *Amphimedon* total RNA, Michael Kube (MPI for Molecular Genetics, Berlin) for *T. wilhelma* transcriptome 454 sequencing, David Fredman and Tsuyoshi Momose for the *C. hemisphaerica* and Tetyana Nosenko for *T. wilhelma* transcriptome assemblies, Heiko Schmidt (MFPL, Vienna) for advice on phylogeny, Benjamin Weiss (Jena) for technical assistance with *T. wilhelma* sections, Genoscope for *C. hemisphaerica* sequencing projects, and the members of the Technau lab for discussion. The research was funded by fellowships of the Austrian Science Fund (FWF): P21108-B17 and the ITN EVONET (project 215781) to U.T., the Australian Research Council to B.M.D., the Alexander von Humboldt Foundation to CL, ANR grant “DiploDevo” to EH and the German Science Foundation (DFG) through the Priority Program 1174 “Deep Metazoan Phylogeny” (Project Wo896/6) to GW.

## References

1. Seipel K, Schmid V. Evolution of striated muscle: Jellyfish and the origin of triploblasty. *Dev Biol.* 2005; 282:14–26. [PubMed: 15936326]
2. Schuchert P, Reber-Müller S, Schmid V. Life stage specific expression of a myosin heavy chain in the hydrozoan *Podocoryne carnea*. *Differentiation.* 1993; 54:11–18. [PubMed: 8104835]
3. Chapman, DM.; Muscatine, L. *Coelenterate Biology.* Lenhoff, HM., editor. Academic Press; New York, San Francisco, London: 1974.
4. Burton PM. Insights from diploblasts; the evolution of mesoderm and muscle. *J Exp Zool (Mol Dev Evol).* 2007; 308B:1–10.
5. Schmidt-Rhaesa, A. *The evolution of organ systems.* Edn. 1. Oxford University Press; 2007.
6. Mackie GO, Mills CE, Singla CL. Structure and function of the prehensile tentilla of *Euplokamis* (Ctenophora, Cydippida). *Zoomorphology.* 1988; 107:319–337.
7. Boelsterli U. An electron microscopic study of early developmental stages, myogenesis, oogenesis, and cnidogenesis in the anthomedusa, *Podocoryne carnea* M. Sars. *Journal of Morphology.* 1977; 154:259–290. [PubMed: 21970]
8. Squire JM, Al-Khayat HA, Knupp C, Luther PK. Molecular architecture in muscle contractile assemblies. *Adv Protein Chem.* 2005; 71:17–87. [PubMed: 16230109]
9. Hooper SL, Hobbs KH, Thuma JB. Invertebrate muscles: thin and thick filament structure; molecular basis of contraction and its regulation, catch and asynchronous muscle. *Progress Neurobiol.* 2008; 86:72–127.
10. Kamm KE, Stull JT. Dedicated myosin light chain kinases with diverse cellular functions. *J Biol Chem.* 2001; 276:4527–4530. [PubMed: 11096123]
11. Korn ED. Coevolution of head, neck, and tail domains of myosin heavy chains. *Proc Natl Acad Sci U S A.* 2000; 97:12559–12564. [PubMed: 11058170]
12. Oota S, Saitou N. Phylogenetic relationship of muscle tissues deduced from superimposition of gene trees. *Mol Biol Evol.* 1999; 16:856–867. [PubMed: 10368962]
13. Goodson HV, Spudich JA. Molecular evolution of the myosin family: Relationships derived from comparisons of amino acid sequences. *Proc Natl Acad Sci U S A.* 1993; 90:659–663. [PubMed: 8421702]
14. Vicente-Manzanares M, Ma X, Adelstein RS, Horwitz AR. Non-muscle myosin II takes centre stage in cell adhesion and migration. *Nat Rev Mol Cell Biol.* 2009; 10:778–790. [PubMed: 19851336]
15. Hooper SL, Thuma JB. Invertebrate muscles: muscle specific genes and proteins. *Physiol Rev.* 2005; 85:1001–1060. [PubMed: 15987801]
16. Nickel M, Scheer C, Hammel JU, Herzen J, Beckmann F. The contractile sponge epithelium sensu lato—body contraction of the demosponge *Tethya wilhelma* is mediated by the pinacoderm. *J Exp Biol.* 2011; 214:1692–1698. [PubMed: 21525315]
17. Hammel, JU. PhD thesis. Friedrich-Schiller-Universität Jena; 2010. Zur Funktion des Wasserleitungssystems und der Entwicklung von Knospen in Schwämmen. Morphologische Grundlagen einer reversen Genetik.



18. Adamska M, et al. Structure and expression of conserved Wnt pathway components in the demosponge *Amphimedon queenslandica*. *Evol Dev*. 2010; 12:494–518. [PubMed: 20883218]
19. Renfer E, Amon-Hassenzahl A, Steinmetz PR, Technau U. A muscle-specific transgenic reporter line of the sea anemone, *Nematostella vectensis*. *Proc Natl Acad Sci U S A*. 2010; 107:104–108. [PubMed: 20018670]
20. Rui Y, Bai J, Perrimon N. Sarcomere formation occurs by the assembly of multiple latent protein complexes. *PLoS Genet*. 2010; 6:e1001208. [PubMed: 21124995]
21. Sanger JM, Sanger JW. The dynamic Z bands of striated muscle cells. *Sci Signal*. 2008; 1:e37.
22. Clark KA, McElhinny AS, Beckerle MC, Gregorio CC. Striated muscle cytoarchitecture: an intricate web of form and function. *Annu Rev Cell Dev Biol*. 2002; 18:637–706. [PubMed: 12142273]
23. Frank D, Kuhn C, Katus HA, Frey N. The sarcomeric Z-disc: a nodal point in signalling and disease. *J Mol Med*. 2006; 84:446–468. [PubMed: 16416311]
24. Martindale MQ, Pang K, Finnerty JR. Investigating the origins of triploblasty: ‘mesodermal’ gene expression in a diploblastic animal, the sea anemone *Nematostella vectensis* (Phylum Cnidaria; Class Anthozoa). *Development*. 2004; 131:2463–2474. [PubMed: 15128674]
25. Ayme-Southgate AJ, Southgate RJ, Philipp RA, Sotka EE, Kramp C. The myofibrillar protein, projectin, is highly conserved across insect evolution except for its PEVK domain. *J Mol Evol*. 2008; 67:653–669. [PubMed: 18982379]
26. Kenny PA, Liston EM, Higgins DG. Molecular evolution of immunoglobulin and fibronectin domains in titin and related muscle proteins. *Gene*. 1999; 232:11–23. [PubMed: 10333517]
27. Sutter SB, Raeker MO, Borisov AB, Russell MW. Orthologous relationship of obscurin and Unc-89: phylogeny of a novel family of tandem myosin light chain kinases. *Dev Genes Evol*. 2004; 214:352–359. [PubMed: 15185077]
28. Craig R, Woodhead JL. Structure and function of myosin filaments. *Curr Opin Struct Biol*. 2006; 16:204–212. [PubMed: 16563742]
29. Torruella G, et al. Phylogenetic relationships within the Opisthokonta based on phylogenomic analyses of conserved single-copy protein domains. *Mol Biol Evol*. 2012; 29:531–544. [PubMed: 21771718]
30. Philippe H, et al. Phylogenomics revives traditional views on deep animal relationships. *Curr Biol*. 2009; 19:706–712. Supplementary References. [PubMed: 19345102]

## Supplementary References

31. Kim HR, Appel S, Vetterkind S, Gangopadhyay SS, Morgan KG. Smooth muscle signalling pathways in health and disease. *J Cell Mol Med*. 2008; 12:2165–2180. [PubMed: 19120701]
32. Farah CS, Reinach FC. The troponin complex and regulation of muscle contraction. *Faseb J*. 1995; 9:755–767. [PubMed: 7601340]
33. Somlyo AP, Somlyo AV. Ca<sup>2+</sup> sensitivity of smooth muscle and nonmuscle myosin II: modulated by G proteins, kinases, and myosin phosphatase. *Physiol Rev*. 2003; 83:1325–1358. [PubMed: 14506307]
34. Nickel M, Donath T, Schweikert M, Beckmann F. Functional morphology of *Tethya* species (Porifera): 1. Quantitative 3D-analysis of *Tethya wilhelma* by synchrotron radiation based X-ray microtomography. *Zoomorphology*. 2006; 125:209–223.
35. Leys SP, Degnan BM. Embryogenesis and metamorphosis in a haplosclerid demosponge: gastrulation and transdifferentiation of larval ciliated cells to choanocytes. *Invertebrate Biology*. 2002; 121:171–189.
36. Klaavuniemi T, Kelloniemi A, Ylännä J. The ZASP-like motif in actinin-associated LIM protein is required for interaction with the  $\alpha$ -actinin rod and for targeting to the muscle Z-line. *J Biol Chem*. 2004; 279:26402–26410. [PubMed: 15084604]
37. Nakagawa N, et al. ENH, containing PDZ and LIM domains, heart/skeletal muscle-specific protein, associates with cytoskeletal proteins through the PDZ domain. *Biochem Biophys Res Commun*. 2000; 272:505–512. [PubMed: 10833443]

38. Ozato K, Shin DM, Chang TH, Morse H.C.r. TRIM family proteins and their emerging roles in innate immunity. *Nat Rev Immunol.* 2008; 8:849–860. [PubMed: 18836477]
39. Björklund ÅK, Light S, Sagit R, Elofsson A. Nebulin: A study of protein repeat evolution. *J Mol Biol.* 2010; 402:38–51. [PubMed: 20643138]
40. Hanashima A, Kubokawa K, Kimura S. Structure of the amphioxus nebulin gene and evolution of the nebulin family genes. *Gene.* 2009; 443:76–82. [PubMed: 19406219]
41. Burkart C, et al. Modular proteins from the *Drosophila* *sallimus* (*sls*) gene and their expression in muscles with different extensibility. *J Mol Biol.* 2007; 367:953–969. [PubMed: 17316686]
42. Kontrogianni-Konstantopoulos A, Ackermann MA, Bowman AL, Yap SV, Bloch RJ. Muscle giants: molecular scaffolds in sarcomerogenesis. *Physiol Rev.* 2009; 89:1217–1267. [PubMed: 19789381]
43. Fritzenwanker JH, Technau U. Induction of gametogenesis in the basal cnidarian *Nematostella vectensis*. *Dev Genes Evol.* 2002; 212:99–103. [PubMed: 11914942]
44. Chevalier S, Martin A, Leclere L, Amiel A, Houliston E. Polarised expression of FoxB and FoxQ2 genes during development of the hydrozoan *Clytia hemisphaerica*. *Dev Genes Evol.* 2006; 216:709–720. [PubMed: 17021866]
45. Leys SP, Degnan BM. Cytological basis of photoresponsive behavior in a sponge larva. *Biol Bull.* 2001; 201:323–338. [PubMed: 11751245]
46. Sarà M, Sarà A, Nickel M, Brümmer F. Three new species of *Tethya* (Porifera: Demospongiae) from German aquaria. *Stuttgarter Beiträge zur Naturkunde.* 2001; A:1–15.
47. Nickel M. Kinetics and rhythm of body contractions in the sponge *Tethya wilhelma* (Porifera: Demospongiae). *J Exp Biol.* 2004; 207:4515–4524. [PubMed: 15579547]
48. Putnam NH, et al. The amphioxus genome and the evolution of the chordate karyotype. *Nature.* 2008; 453:1064–1071. [PubMed: 18563158]
49. Putnam NH, et al. Sea anemone genome reveals ancestral eumetazoan gene repertoire and genomic organization. *Science.* 2007; 317:86–94. [PubMed: 17615350]
50. Chapman JA, et al. The dynamic genome of *Hydra*. *Nature.* 2010; 464:592–596. [PubMed: 20228792]
51. Ryan JF, et al. The homeodomain complement of the ctenophore *Mnemiopsis leidyi* suggests that Ctenophora and Porifera diverged prior to the ParaHoxozoa. *Evodevo.* 2010; 1:9. [PubMed: 20920347]
52. Srivastava M, et al. The Trichoplax genome and the nature of placozoans. *Nature.* 2008; 454:955–960. [PubMed: 18719581]
53. Srivastava M, et al. The Amphimedon queenslandica genome and the evolution of animal complexity. *Nature.* 2010; 466:720–726. [PubMed: 20686567]
54. King N, et al. The genome of the choanoflagellate *Monosiga brevicollis* and the origin of metazoans. *Nature.* 2008; 451:783–788. [PubMed: 18273011]
55. Ruiz-Trillo I, et al. The origins of multicellularity: a multi-taxon genome initiative. *Trends Genet.* 2007; 23:113–118. [PubMed: 17275133]
56. Merchant SS, et al. The *Chlamydomonas* genome reveals the evolution of key animal and plant functions. *Science.* 2007; 318:245–250. [PubMed: 17932292]
57. Banks JA, et al. The *Selaginella* genome identifies genetic changes associated with the evolution of vascular plants. *Science.* 2011; 332:960–963. [PubMed: 21551031]
58. Eichinger L, et al. The genome of the social amoeba *Dictyostelium discoideum*. *Nature.* 2005; 435:43–57. [PubMed: 15875012]
59. Fritz-Laylin LK, et al. The genome of *Naegleria gruberi* illuminates early eukaryotic versatility. *Cell.* 2010; 140:631–642. [PubMed: 20211133]
60. Fernandez-Fueyo E, et al. Comparative genomics of *Ceriporiopsis subvermispora* and *Phanerochaete chrysosporium* provide insight into selective ligninolysis. *Proc Natl Acad Sci U S A.* 2012; 20
61. Wood V, et al. The genome sequence of *Schizosaccharomyces pombe*. *Nature.* 2002; 415:871–880. [PubMed: 11859360]

62. Burge C, Karlin S. Prediction of complete gene structures in human genomic DNA. *J Mol Biol.* 1997; 268:78–94. [PubMed: 9149143]
63. Shinzato C, et al. Using the *Acropora digitifera* genome to understand coral responses to environmental change. *Nature.* 2011; 476:320–323. [PubMed: 21785439]
64. Hunter S, et al. InterPro: the integrative protein signature database. *Nucleic Acids Res.* 2009; 37:D211–215. [PubMed: 18940856]
65. Finn RD, et al. The Pfam protein families database. *Nucleic Acids Res.* 2009; 38:D211–222. [PubMed: 19920124]
66. Lupas A, Van Dyke M, Stock J. Predicting coiled coil from protein sequences. *Science.* 1991; 252
67. Edgar RC. MUSCLE: multiple sequence alignment with high accuracy and high throughput. *Nucleic Acids Res.* 2004; 32:1792–1797. [PubMed: 15034147]
68. Castresana J. Selection of conserved blocks from multiple alignments for their use in phylogenetic analysis. *Mol Biol Evol.* 2000; 17:540–552. [PubMed: 10742046]
69. Abascal F, Zardoya R, Posada D. ProtTest: Selection of best-fit models of protein evolution. *Bioinformatics.* 2005; 21:2104–2105. [PubMed: 15647292]
70. Thompson JD, Gibson TJ, Plewniak F, Jeanmougin F, Higgins DG. The ClustalX windows interface: flexible strategies for multiple sequence alignment aided by quality analysis tools. *Nucl. Acids Res.* 1997; 24:4876–4882. [PubMed: 9396791]
71. Guindon S, et al. New algorithms and methods to estimate maximum-likelihood phylogenies: assessing the performance of PhyML 3.0. *Systematic Biology.* 2010; 59:307–321. [PubMed: 20525638]
72. Altekar G, Dwarkadas S, Huelsenbeck JP, Ronquist F. Parallel Metropolis-coupled Markov chain Monte Carlo for Bayesian phylogenetic inference. *Bioinformatics.* 2004; 20:407–415. [PubMed: 14960467]
73. Ronquist F, Huelsenbeck JP. MRBAYES 3: Bayesian phylogenetic inference under mixed models. *Bioinformatics.* 2003; 19:1572–1574. [PubMed: 12912839]
74. Genikhovich G, Technau U. *In situ* hybridization of starlet sea anemone (*Nematostella vectensis*) embryos, larvae, and polyps. *Cold Spring Harb Protoc.* 2009; 2009 pdb prot5282.
75. Larroux C, et al. Developmental expression of transcription factor genes in a demosponge: insights into the origin of metazoan multicellularity. *Evol Dev.* 2006; 8:150–173. [PubMed: 16509894]
76. Larroux C, et al. Whole-mount in situ hybridization in *Amphimedon*. *CSH Protoc.* 2008; 2008 pdb prot5096.
77. Hammel JU, Herzen J, Beckmann F, Nickel M. Sponge budding is a spatiotemporal morphological patterning process: Insights from synchrotron radiation-based x-ray microtomography into the asexual reproduction of *Tethya wilhelma*. *Front Zool.* 2009; 6:19. [PubMed: 19737392]
78. Weissenfels N. Scanning electron microscope histology of spongy *Ephydatia fluviatilis*. *Microsc Acta.* 1982; 85:345–350.

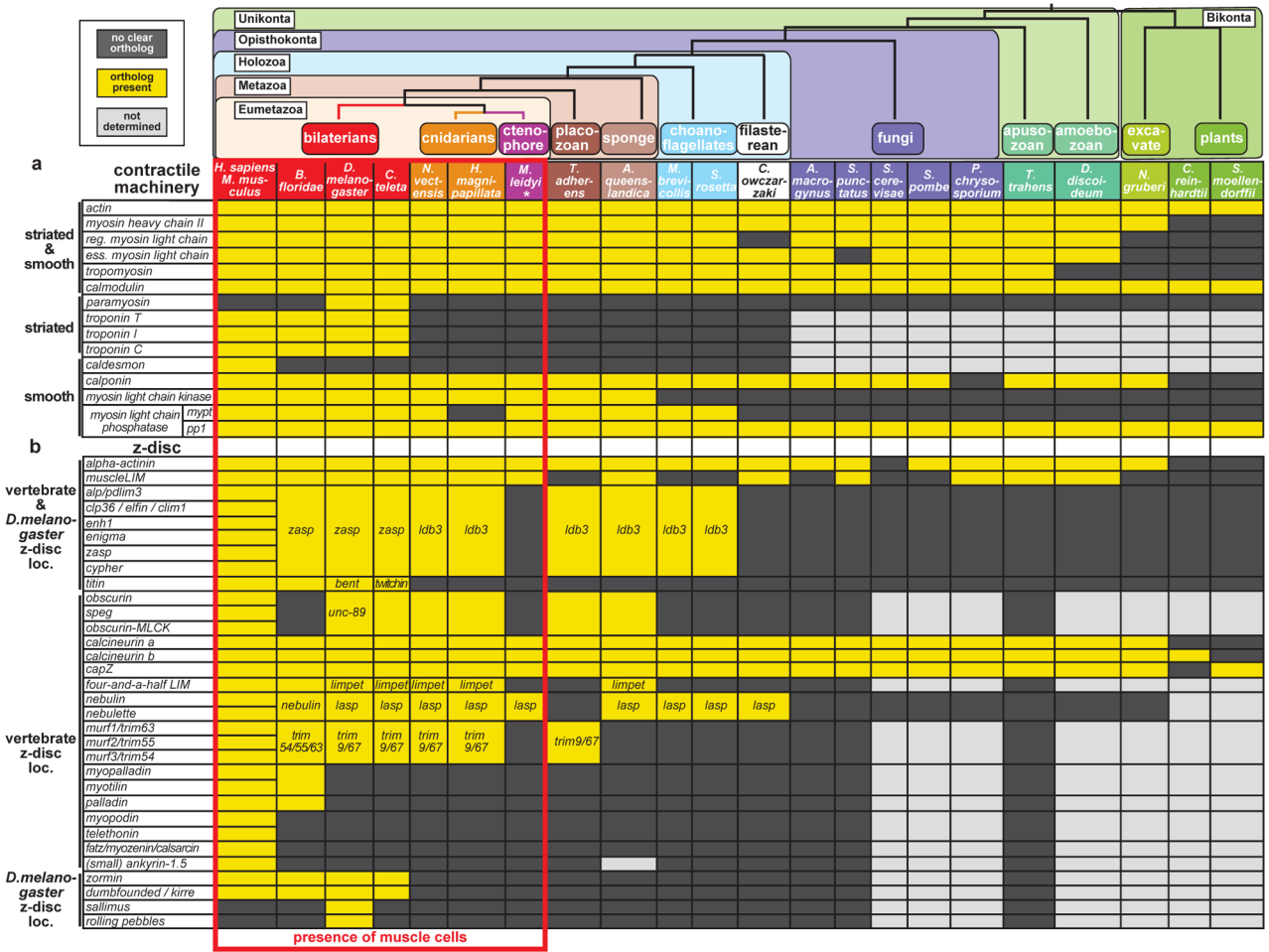


**Figure 1. Complex phylogenomic distribution of contractile machinery (a) and z-disc interactome (b) components**

Rows: gene names of vertebrate and/or *D. melanogaster* contractile machinery (a) or z-disc complex (b) components. Columns: species and their phylogenetic relationship<sup>29, 30</sup>.

Asterisk: only a preliminary assembly without gene predictions was available for *M. leidy*.

Row labels in (a): site of predominant gene expression; in (b): species with reported z-disc localization of the gene product. Multifamily protein and uncertain orthologies supported by further molecular phylogenetic and protein domain analyses (Supplementary Figs. 2, 6, 7).

All abbreviations in Supplementary Table 1.

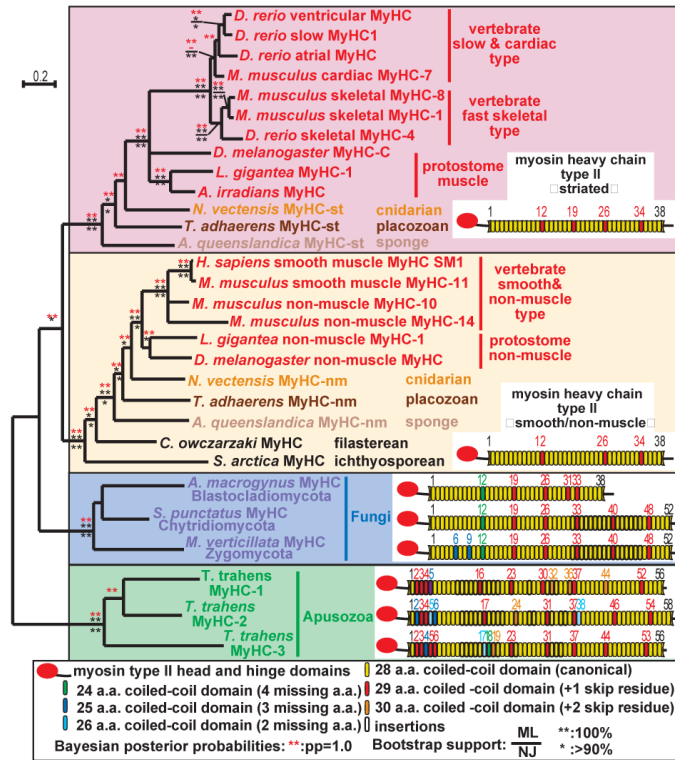


**Figure 2. Ancient *myhc* gene duplication predated animal radiation**

Maximum likelihood phylogenetic tree of MyHC type II proteins with nodes collapsed if they diverged between neighbour-joining, maximum likelihood, or Bayesian inference. The nesting of protist MyHCs within the MyHC-nm orthology group supports a *myhc* duplication event in the common ancestor of Metazoa, Choanoflagellata, Filasterea and Ichthyosporea, but also assumes secondary losses of *myhc-st* genes in protist phyla. Diagrams: MyHC domain structures. Final alignment length: 1730 a.a. Scale bar: 0.2 changes per site. Coloured numbers: positions of non-canonical coiled-coil domains. a.a.: amino acid. Species abbreviations, sequence accession and protein model numbers in Supplementary Table 1.

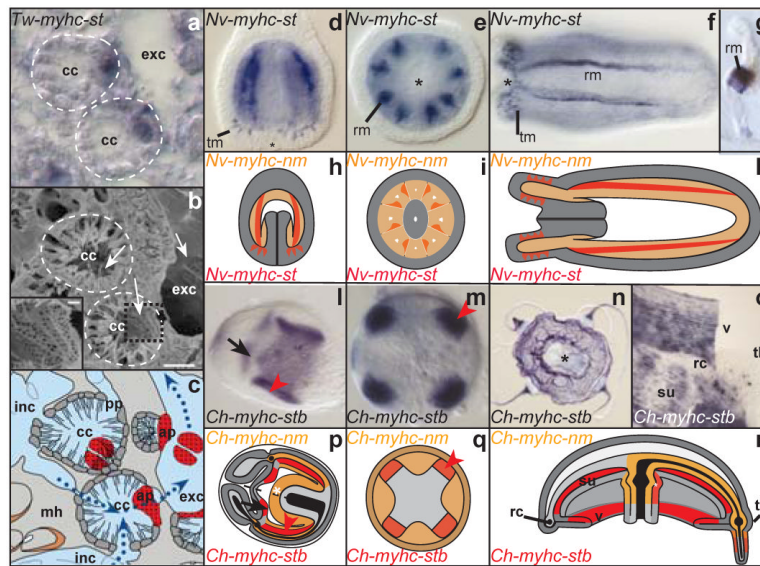


**Figure 3. Expression of *myhc-st* in a demosponge, and in anthozoan and hydrozoan cnidarians**  
*In situ* hybridisations (a, d-g, l-o) and schematic representations (c, h-k, p-r) of *myhc-st* expression in the adult demosponge *Tethya wilhelma* (a,c), the anthozoan *Nematostella vectensis* (d-k), and the hydrozoan *Clytia hemisphaerica* (l-r). Scanning electron microscopy image (b) and schematic representation (c) of a sectioned choanocyte chambers of *T. wilhelma*. *Tw-myhc-st*-expressing multi-porous cells (b, white arrows, inlet; c, red) are likely involved in water flow (blue dotted arrows) regulation through choanocyte chambers (within dotted white lines). (o) Velum of a young medusa was lifted. Developmental stages: (d-e, h-i) 4 days old planula; (f,k) 9 days old primary polyps; (l-m, p-q) medusal buds; (n-o, r) young medusae; (a-c, g) adults. (a,g) Cross-sections of stained animals; (d-g, l-o) whole-mount micrographs. Views: (d,f,h,k-l,p,r) lateral; (e,i, m-o,q) oral. Aboral towards top (d,h,r) or lower-right (f, k-l, p). Asterisk: mouth. ap: apopyle; cc: choanocyte chamber; exc: excurrent channel; inc: incurrent channel; mh: mesohyl; pp: prosopyle; rc: ring canal; rm: retractor muscle; su: subumbrella; tb: tentacle bulb; tm: tentacle muscle; v: velum. Scale bar: 10 $\mu$ m.

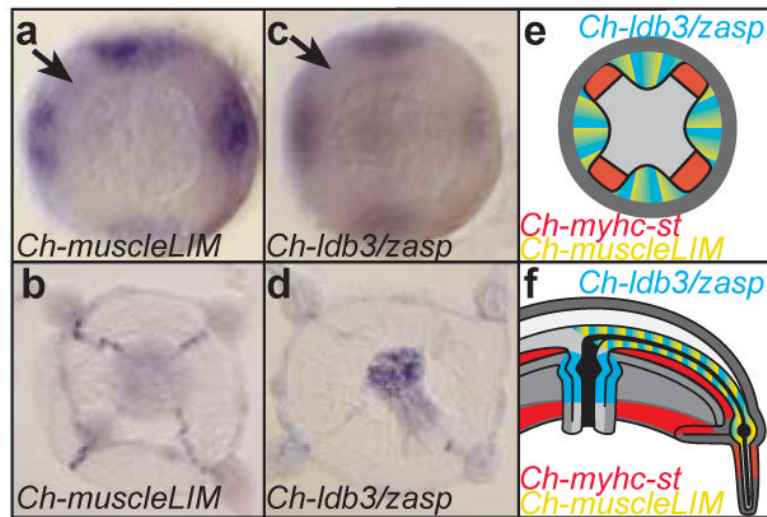


**Figure 4. Absence of *Clytia hemisphaerica* *muscleLim* and *Ch-ldb3/zasp* expression in striated muscles**

*In situ* hybridisation (a-d) and schematic representation (e-f) of *Ch-muscleLim* (a, b), *Ch-ldb3/zasp* (c, d) expression mainly restricted to the developing radial canal endoderm (a-f). *Ch-myhc-st*-positive subumbrella striated muscle precursor cells (arrows, compare with Fig. 3m) do not show *muscleLim*- or *ldb3/zasp*-expression. Stages: medusal bud (a,c,e), young medusa (b,d,f). All oral views.